



HAL
open science

Oxygen history off Baja California over the last 80 kyr: A new foraminiferal-based record

Martin Tetard, Laetitia Licari, Luc L Beaufort

► To cite this version:

Martin Tetard, Laetitia Licari, Luc L Beaufort. Oxygen history off Baja California over the last 80 kyr: A new foraminiferal-based record. *Paleoceanography*, 2017, 32 (3), pp.246 - 264. 10.1002/2016PA003034 . hal-01514644

HAL Id: hal-01514644

<https://hal.science/hal-01514644>

Submitted on 1 Dec 2021

HAL is a multi-disciplinary open access archive for the deposit and dissemination of scientific research documents, whether they are published or not. The documents may come from teaching and research institutions in France or abroad, or from public or private research centers.

L'archive ouverte pluridisciplinaire **HAL**, est destinée au dépôt et à la diffusion de documents scientifiques de niveau recherche, publiés ou non, émanant des établissements d'enseignement et de recherche français ou étrangers, des laboratoires publics ou privés.

Copyright



RESEARCH ARTICLE

10.1002/2016PA003034

Oxygen history off Baja California over the last 80 kyr: A new foraminiferal-based record

Martin Tetard¹ , Laetitia Licari¹ , and Luc Beaufort¹ ¹Aix-Marseille Université, CNRS, IRD, CEREGE UM34, Aix-en-Provence, France

Key Points:

- Relative abundances of benthic foraminiferal assemblages were used to quantify [O₂] over the last glacial in the eastern Pacific Ocean
- The estimated oxygen record correlates well with global climate changes (low [O₂] during warm episodes and high [O₂] during cold periods)
- Relative abundances of benthic foraminiferal assemblages were used to quantify [O₂] over the last glacial in the eastern Pacific Ocean

Supporting Information:

- Supporting Information S1
- Data Set S1
- Table S1

Correspondence to:

M. Tetard,
tetard@cerge.fr

Citation:

Tetard, M., L. Licari, and L. Beaufort (2017), Oxygen history off Baja California over the last 80 kyr: A new foraminiferal-based record, *Paleoceanography*, 32, 246–264, doi:10.1002/2016PA003034.

Received 7 SEP 2016

Accepted 12 FEB 2017

Accepted article online 20 FEB 2017

Published online 11 MAR 2017

Abstract The intensity of the Oxygen minimum zone (OMZ) of the eastern North Pacific (ENP) experienced strong variations during the last glacial, mirroring changes in the balance between export production (O₂ consumption) and water mass ventilation (O₂ renewal). In this paper we present a new benthic foraminiferal assemblages record from Core MD02-2508, recovered from the Pacific slope off Baja California, Mexico. The record reflects oxygen conditions at the northern limit of the OMZ during the last 80 kyr. We statistically identified three assemblages, characteristic of dysoxic, suboxic, and oxic conditions, which we used to produce the first semiquantitative reconstruction of [O₂] for the northeastern Pacific Ocean. Our results show that the estimated [O₂] covaries with δ¹⁸O records from the North Greenland Ice Core Project. Oxygen concentrations overall exhibit moderate values (~1 mL.L⁻¹) during stadials, reaching ~2 mL.L⁻¹ during stadials corresponding to Heinrich events in the Atlantic Ocean. Conversely, bottom waters at the core location were strongly depleted in oxygen (<0.5 mL.L⁻¹) during interstadials. Benthic foraminiferal abundance increased with higher export production as recorded by geochemical tracers (Cd/Al ratio). This export production signal increases (decreases) with a fall (rise) in [O₂] during interstadials (stadials), suggesting a relationship between both parameters during these intervals. The influence of ventilation on oxygenation is also a key player. O₂ pulses suggested by the downcore records of serial/spiral test ratio and abundance of oxic species may be explained by enhanced ventilation during Heinrich stadials, in agreement with latest modeling-based oceanic circulation reconstructions.

1. Introduction

Oxygen minimum zones (OMZs) are subsurface water masses characterized by dissolved oxygen content permanently below 0.5 mL.L⁻¹ [Helly and Levin, 2004; Paulmier and Ruiz-Pino, 2009]. In a context of future increases in OMZ volume linked to modern global warming [Stramma et al., 2008; Scholz et al., 2014; Moffitt et al., 2015a], understanding the dynamics of these areas remains of prime interest. In the modern ocean, one of the most intense OMZs is located in the eastern North Pacific (ENP) [Paulmier and Ruiz-Pino, 2009]. While a combined role of high productivity, slow ventilation, and reduced oxygen solubility is assumed to explain the formation of the modern ENP OMZ [Wyrski, 1962; Helly and Levin, 2004; Dean et al., 2006; van Geen et al., 2006; Paulmier and Ruiz-Pino, 2009; Praetorius et al., 2015], several studies indicate that single changes in either production [Phleger and Soutar, 1973; Crusius et al., 2004; Ortiz et al., 2004] or oceanic circulation [Cannariato et al., 1999; Zheng et al., 2000; Schmittner et al., 2007] could explain variations in the OMZ intensity as recorded in the past, although the relative importance of both processes remains elusive.

During the last glacial, OMZ strength followed centennial- to millennial-scale climate oscillations known as Dansgaard-Oeschger (DO) events, first documented by Dansgaard et al. [1993] in ice cores from Greenland, and Heinrich (H) events, corresponding to disrupted global thermohaline circulation caused by major ice sheet collapses sending massive freshwater pulses into the North Atlantic [Heinrich, 1988; Sigman et al., 2007]. Both types of events have a strong impact on global climate and oceanic circulation [e.g., Timmermann et al., 2005]. In the northeastern Pacific, they are translated into oxygen content fluctuations [Cannariato and Kennett, 1999; Schmittner et al., 2007]. During the last few decades, a number of studies have been conducted at several locations along the California Coast (Point Concepción [Cannariato and Kennett, 1999], Santa Barbara basin (SBB) [Bernhard and Reimers, 1991; Cannariato et al., 1999; Hendy and Kennett, 2000; Ortiz et al., 2004; van Geen et al., 2006; Moffitt et al., 2014], and off Mazatlan coast [Nameroff et al., 2002]). However, the southern part of Baja California, located southward closer to the core of the OMZ, remains much less studied than the Santa Barbara basin [e.g., Dean et al., 2006; Cartapanis et al., 2011, 2014]. While most available studies off Baja California focused on geochemical tracers (MD02-2508 [Cartapanis et al., 2011, 2014],

NH15P [Nameroff *et al.*, 2002], and PC08 and PC10 [Dean *et al.*, 2006]), in this paper we present the first semi-quantitative record of $[O_2]$ off Baja California during the last 80 kyr using a micropaleontological approach based on assemblages of benthic foraminifera from Core MD02-2508. This record adds knowledge to the paleo-oxygenation latitudinal transect along the northeastern Pacific Coast (Figure 1) and helps to decipher the main drivers involved in past ENP OMZ dynamics.

Benthic foraminifera are sensitive tracers of trophic and oxygen conditions at the bottom of the water column [e.g., Jorissen *et al.*, 1995], and analysis of rapid modifications in their fossil assemblages have been successfully used to reconstruct short time-scale paleoceanographical changes along the northern part of the ENP margin [Bernhard and Reimers, 1991; Cannariato and Kennett, 1999; Cannariato *et al.*, 1999]. Dissolved oxygen content of bottom and pore waters is generally assumed to be the main factor limiting the distribution of benthic foraminifera in OMZs [Oberhänsli *et al.*, 1990; Loubere, 1994; Den Dulk *et al.*, 1998, 2000; Schumacher *et al.*, 2007; Caille *et al.*, 2015]. Indeed, in modern OMZs (e.g., Arabian Sea; Peru), some species, such as *Bolivina seminuda*, are associated with the core region and respond rapidly and gradually to $[O_2]$ while others, such as *Uvigerina peregrina*, are found below the core in more oxygenated environments [Caille *et al.*, 2014]. These microorganisms are thus essential tools for reconstructing past spatial and temporal variations of OMZs [Moffitt *et al.*, 2015a] as the relative dominance of some assemblages can reflect extension or contraction of the OMZ core [Oberhänsli *et al.*, 1990; Koho and Piña-Ochoa, 2012; Mallon *et al.*, 2012].

2. Materials and Methods

2.1. Studied Core

Core MD02-2508 (23°27.91'N, 111°35.74'W; 40.42 m long) was recovered at a water depth of 606 m on the continental slope ~90 km off the coast of Baja California Sur, Mexico, during the R/V *Marion-Dufresne* MD126 MONA (Image VII) campaign in 2002. The coring site is located on the edge of the ENP OMZ core [Helly and Levin, 2004; Cartapanis *et al.*, 2011]. Current mean annual oxygen level is $\sim 0.13 \text{ mL L}^{-1}$ at the core location (Figure 1) [Garcia *et al.*, 2014].

The age model of Core MD02-2508 was previously established using radiocarbon dating (^{14}C) of foraminifera, magnetic excursion (i.e., Blake) [Blanchet *et al.*, 2007], and refined with visual correlation between wet bulk density and North Greenland Ice Core Project (NGRIP) oxygen isotope record (Figure 2) [Cartapanis *et al.*, 2011, 2014]. Core MD02-2508 extends from 0 to 120 ka, with an average sedimentation rate ranging from 18 cm/kyr (during the Last Glacial Maximum (LGM)) to 44 cm/kyr (during the Holocene [Cartapanis *et al.*, 2011]). The sediments are alternatively composed of nonlaminated hemipelagic silty-clayey muds, containing biogenic and minerogenic fractions and bearing bioturbation marks, and laminated intervals. Those millimeter to centimeter scale laminae exhibit alternating whitish biogenic compounds (e.g., diatoms and/or foraminiferal tests), and blackish organic and terrigenous compounds [Blanchet *et al.*, 2007; Murdmaa *et al.*, 2010], which are almost devoid of any foraminiferal test.

2.2. Oceanographic Settings

Coring site MD02-2508 is ideal for investigating variations in intensity of the OMZ off California, as it is not located directly within the OMZ core, which is supposed to have been relatively stable over the Holocene time [Koho and Piña-Ochoa, 2012]. OMZ variations are due to the equilibrium between the oxygenated and productive southward water masses, and the dysoxic and sluggish currents flowing northward and mixing off Baja California [Zheng *et al.*, 2000; van Geen *et al.*, 2006; Herguera *et al.*, 2010]. The northern cold and oxygenated water mass corresponds to the sub-Arctic water transported at the surface by the California Current [Durazo, 2015; Lynn and Simpson, 1987] and to the North Pacific Intermediate Water (NPIW) down to 1000 m [Durazo and Baumgartner, 2002]. These water bodies are gradually depleted in oxygen content as they are transported southward due to the combined effects of organic carbon export consuming O_2 and progressive mixing with the dysoxic water masses flowing northward [Paulmier and Ruiz-Pino, 2009]. This northward subsurface and oxygen-depleted water mass, called Equatorial Subsurface Waters (ESSW), is transported by the seasonally varying California Undercurrent [Durazo, 2015; Lynn and Simpson, 1987]. It originates from warm, productive, and highly saline waters undergoing a slow transport to the north along the West Coast of North America (Figure 1) [Cartapanis *et al.*, 2011; Herguera *et al.*, 2010].

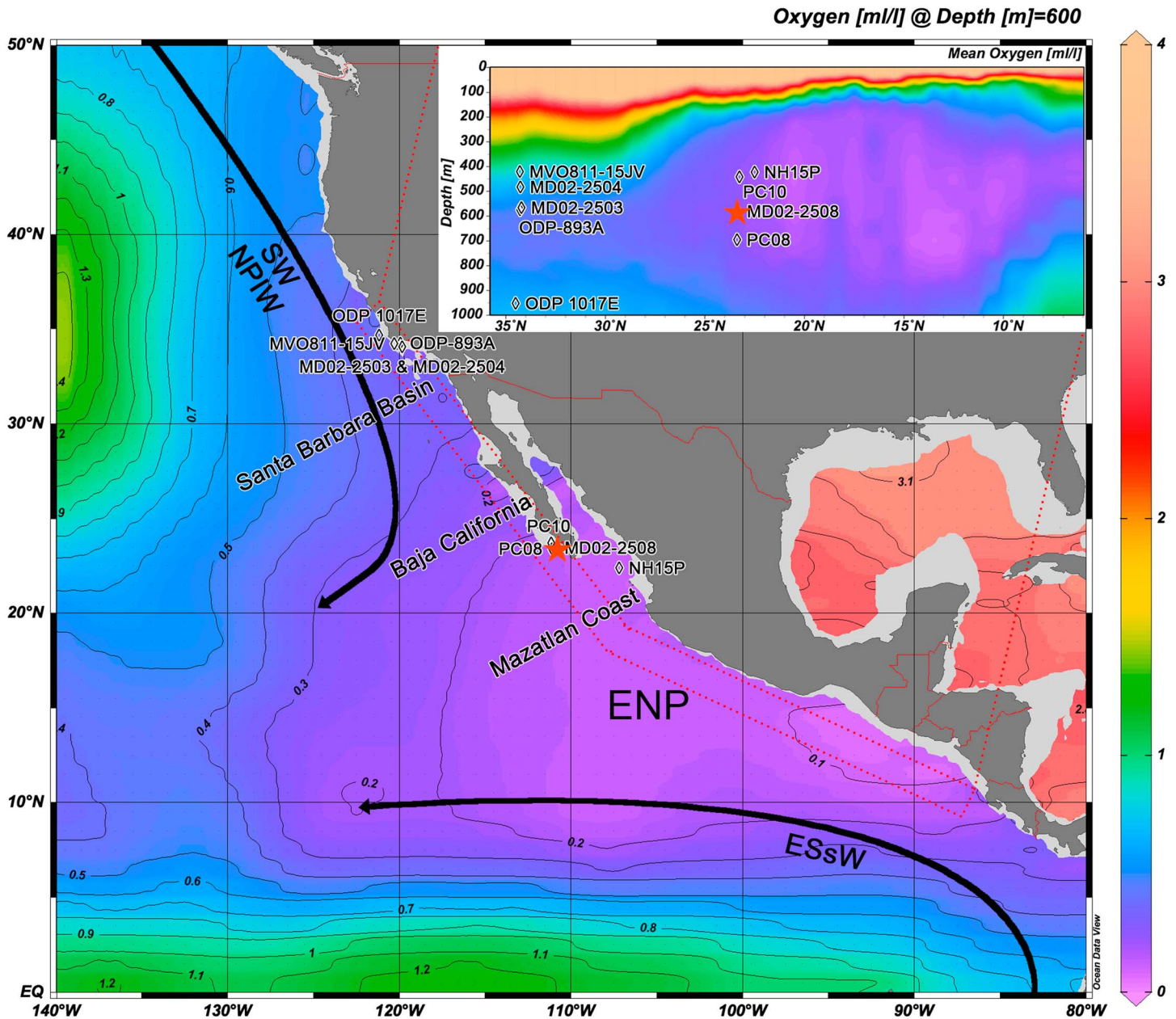


Figure 1. Mean annual dissolved oxygen gradient (mLL^{-1}) at a depth of 600 m off the West Coast of North and central America. The red star shows the location of the core, off Baja California. the inset graph shows the oxygen gradient above the MD02-2508 station. This figure was created by using the Ocean Data View software [Schlitzer, 2017] (<http://odv.awi.de>) and the World Ocean Atlas 2013 data set [Garcia et al., 2014] (<http://www.nodc.noaa.gov/OC5/woa13/>).

Lynn and Simpson, 1987]. Altogether, these water masses are responsible for the formation of the largest OMZ in the world. It accounts for 68% of the global OMZ and is divided into an eastern tropical North Pacific (ETNP: 41%) component, extending from 0° to 25°N, and an eastern subtropical North Pacific (ESTNP: 27%) component, stretching from 25°N to 52°N [Paulmier and Ruiz-Pino, 2009; Cartapanis et al., 2011]. Core MD02-2508 is located between the ETNP, influenced by the ESsW, and the ESTNP, dominated by the NPIW. Variations in the intensity of surface productivity and intermediate ventilation of both surrounding water masses thus impact the coring site. Sediments at this position record alternating periods of cold, oxygen-enhanced conditions and warm, oxygen-depleted conditions [Cannariato and Kennett, 1999; Hendy and Kennett, 2000; Dean et al., 2006], providing evidence for major climatic shifts well recorded in Greenland [Behl and Kennett, 1996; Rodriguez-Sanz et al., 2013].

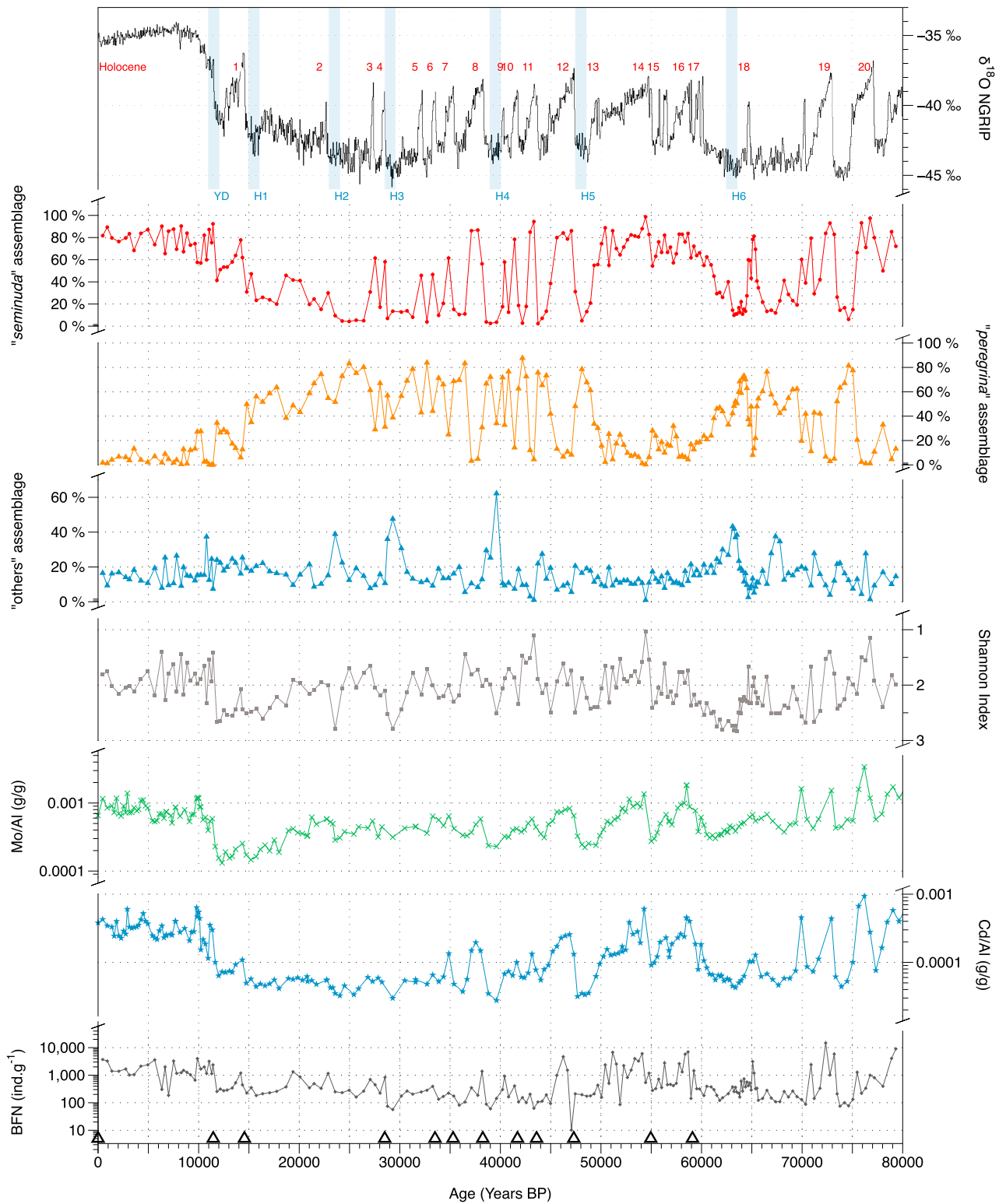


Figure 2. Isotopic composition of the NGRIP ice core [Johnsen et al., 2001], showing the relative abundance of the *seminuda* assemblage, composed of *B. seminuda*, *B. subadvena*, *B. tenuata*, *T. delicata*, the *peregina* assemblage, composed of *U. peregina*, *B. argentea*, *B. spissa*, *E. smithi*, and the others assemblage consisting of the remaining species. Also shown is the Shannon index, reflecting diversity changes within the benthic foraminiferal fauna, the Mo/Al and Cd/Al ratios from Cartapanis et al. [2011, 2014], and the normalized Benthic Foraminiferal Number (BFN: ind g⁻¹), reflecting the absolute abundance of benthic foraminifera. Hollow triangles represent tie points (NGRIP visual correlation) used to develop the age model of Core MD02-2508 [from Cartapanis et al., 2011, 2014] from left to right: respective depth of 0, 500, 592, 892, 980, 1014, 1082, 1168, 1218, 1306, 1514, and 1656 cm.

2.3. Sample Preparation and Benthic Foraminifera Extraction

For benthic foraminifera investigation, samples were prepared according to the following standard procedure: (1) 1 cm thick sediment slices were sampled and wet weighed. (2) Samples were subsequently oven dried at 50°C for 48 h and dry weighed. (3) Samples were then mixed with tap water in order to desegregate and then wet sieved over a screen of 63 μm . (4) The > 63 μm residues were oven dried for 24 h and weighed again. (5) The > 63 μm fraction was dry sieved over a 150 μm screen. (6) Both 63–150 μm and > 150 μm fractions were weighed.

Benthic foraminifera were investigated in the coarse fraction (>150 μm) at a sampling resolution of 10 to 20 cm, which represents an average time resolution of 450 years between each sample. To constrain the succession of faunas during an interval characterized by a significant change in $[\text{O}_2]$, higher-resolution analysis was constrained to the interval corresponding to the DO18 event, as this event is isolated and brief, and the distinct transition to the following H6 event was clearly visible in the core. In this case, samples were taken every 5 cm. In all samples, 300 benthic foraminifera specimens were picked whenever possible from the sediment aliquots (a single sample only contained 108 specimens after a complete picking). This lower limit is recognized as necessary to produce a statistically reliable and detailed quantitative data set [Buzas, 1990; Fatela and Taborda, 2002] where abundant species may only represent 10% of the assemblage [Patterson and Fishbein, 1989]. An individual rarefaction test [Krebs, 1999] in the PAST software, version 3.04 [Hammer et al., 2001], confirmed that 300 specimens was a statistically reliable number (Figure S1 in the supporting information). Every specimen was counted and identified down to the species level. Among these species, very few of them might be concerned by taxonomical issues, and in need of revision or synonymization as the taxonomical species identification is relatively homogeneous among the California coast. Specimens of the most abundant species were metal coated (Au/Pd) and imaged with a scanning electron microscope (SEM; Figure S2).

2.4. Statistical Analysis

As a preliminary approach, a principal component analysis (PCA) was performed on the complete data set to identify the most significant species, as the PCA loadings take their relative abundance into account [Hammer, 2014]. In a second step, a correspondence analysis (CA) was used to gather the samples according to their faunal composition and to investigate the taxonomic composition of samples in response to ecological trends. The aim of this analysis was to enable samples to be ordered along axes coded for environmental gradients and thus plot the taxa onto this same coordinate system in order to understand their distribution with regard to these ecological parameters [Hammer, 2014]. Both statistical analyses (PCA and CA) were computed by using the PAST software, version 3.04 [Hammer et al., 2001], available at <http://folk.uio.no/ohammer/past/>.

2.5. Faunal Descriptors and Tracers

For each sample, the total number of specimens was normalized by investigated aliquot and sediment mass to estimate the benthic foraminiferal number (BFN), expressed as ind g^{-1} . Foraminiferal density is known to respond to the intensity of organic matter input to the seafloor [Herguera and Berger, 1991; Herguera, 1992]. Therefore, this BFN should track changes in export productivity, even if only qualitatively.

Relative abundance of the most important species, statistically grouped into several assemblages, was estimated as well. We also investigated diversity patterns: each sample was analyzed with regard to species diversity, taking into account the number of taxa as well as their relative abundance [Gotelli and Chao, 2013]. For the diversity estimation we used the Shannon index, calculated using the formula [Magurran, 2004; Morris et al., 2014]:

$$\text{Shannon index} = - \sum (n_i/n) \ln (n_i/n),$$

where n_i is the number of individuals of each species i , and n is the total number of individuals.

Among diversity indices, the Shannon index usually displays the most significant patterns [Morris et al., 2014]. It also allows direct comparison to other studies as it is widely used in most foraminiferal studies [Murray, 2006]. The Simpson index, Equitability, Hill index and E241 (number of species for every sample normalized for 241 specimens total, corresponding to the lower end of the number of individuals picked after splitting) were also calculated, but due to their high similarity with the Shannon index will not be discussed herein. The

serial/spiral benthic foraminiferal test ratio (defined as the number of serial tests divided by the number of (serial + spiral) tests and expressed in percent) was investigated as a potential indicator of enhanced ventilation [Murray, 2006]. Foraminiferal data were compared to geochemical records of molybdenum/aluminium (Mo/Al) and cadmium/aluminium (Cd/Al) ratios (g/g), previously investigated in Core MD02-2508 by Cartapanis *et al.* [2011, 2014] and assumed to mirror oxygenation and export production, respectively. Element/aluminium ratios were calculated to consider the influence of terrigenous inputs [Cartapanis *et al.*, 2011].

3. Results

3.1. Data Reliability

A total of 188 samples were investigated for their benthic foraminiferal content, from which we identified 96 species (census data are available in Data Set S1). The potential influence of the quality and quantity of organic carbon supply on the abundance of some species is known and cannot be excluded [Diz and Barker, 2016]. In OMZ area, where food availability is usually not considered as a limiting factor for population growth, benthic foraminiferal distribution mainly depends on bottom water oxygenation [Jorissen *et al.*, 1995, 2007]. However, this nutrient flux to the sea floor is likely to display a growing influence on benthic foraminiferal faunas during oxic conditions, when [O₂] is not limiting anymore [Diz and Barker, 2016].

No bias seems to have been introduced by dissolution or breakage of tests, as most samples display well-preserved specimens, with almost no whitening, opaqueness, or perforation [Ortiz *et al.*, 2004]. Tests were sometimes slightly broken and were ~90% preserved according to the preservation scale defined in Nguyen *et al.* [2009]. We are thus confident that the potential bias that might be induced by carbonates preservation between well-oxygenated and oxygen-depleted intervals (usually leading to an enhanced preservation) is of minor importance.

Individual rarefaction shows that less than 100 individuals are needed to obtain a reliable description of the assemblage for the samples exhibiting low diversity (see details in Figure S1). However, for the few samples with a higher diversity, the plateau is still not reached after more than 300 specimens. Thus, we did not pick any more individuals for these samples, as around 1000 specimens would probably be required, according to Patterson and Fishbein [1989]. An average of 344 specimens per sample was picked, which was enough to reach a plateau and to be used for reliable statistical analyses. Trends described by the relative abundance of the assemblages are smoothed by the low sedimentation rate and therefore considered to represent an annual to pluridecadal mean of faunal variability. Seasonality of foraminiferal abundance and diversity is lost due to the centimeter thickness of samples [Bernhard and Reimers, 1991] as 1 cm ≈ 30 years (average down-core value). In OMZs, however, benthic foraminifera are supposed to be concentrated in the top centimeter layer of sediment, as most of the intermediate and deep infaunal taxa migrate to the surface during stressful conditions [Jorissen *et al.*, 1995; Caille *et al.*, 2015]. This limits potential bias introduced by the mixing of deep dwelling species living several centimeters under the water-sediment interface, with shallow infaunal individuals that may be already dead for several decades or even centuries [Bernhard, 1992]. By contrast, this mixing is still likely to occur during the rare well-oxygenated intervals recorded in Core MD02-2508. Overall, we are confident that benthic foraminiferal tests found in each sediment slice can be considered to be contemporaneous.

3.2. Statistical Identification of Foraminiferal Assemblages

The PCA shows that seven species are well distributed along the first component, PC1 (51.66% of the variance; loadings corresponding to the relative significance of each species for this analysis are given in Table S1). These species are distributed into two groups: (1) one with positive loadings, composed of *Buliminella tenuata*, *Bolivina subadvena*, *Bolivina seminuda*, and *Takayanagia delicata* and (2) one with negative loadings, containing *Bolivina spissa*, *Uvigerina peregrina*, and *Epistominella smithi*. Even though *Bolivina argentea* displays a relatively low negative score for PC1, we decided to consider it as a main species due to its high relative abundance in some samples and high-loading score for the second component, PC2 (Table S1).

Subsequently, the CA was used to plot these eight main species on two axes supposedly related to environmental parameters (Figure 3) and explaining 25.96% and 10.16% of the variance, respectively. Both species

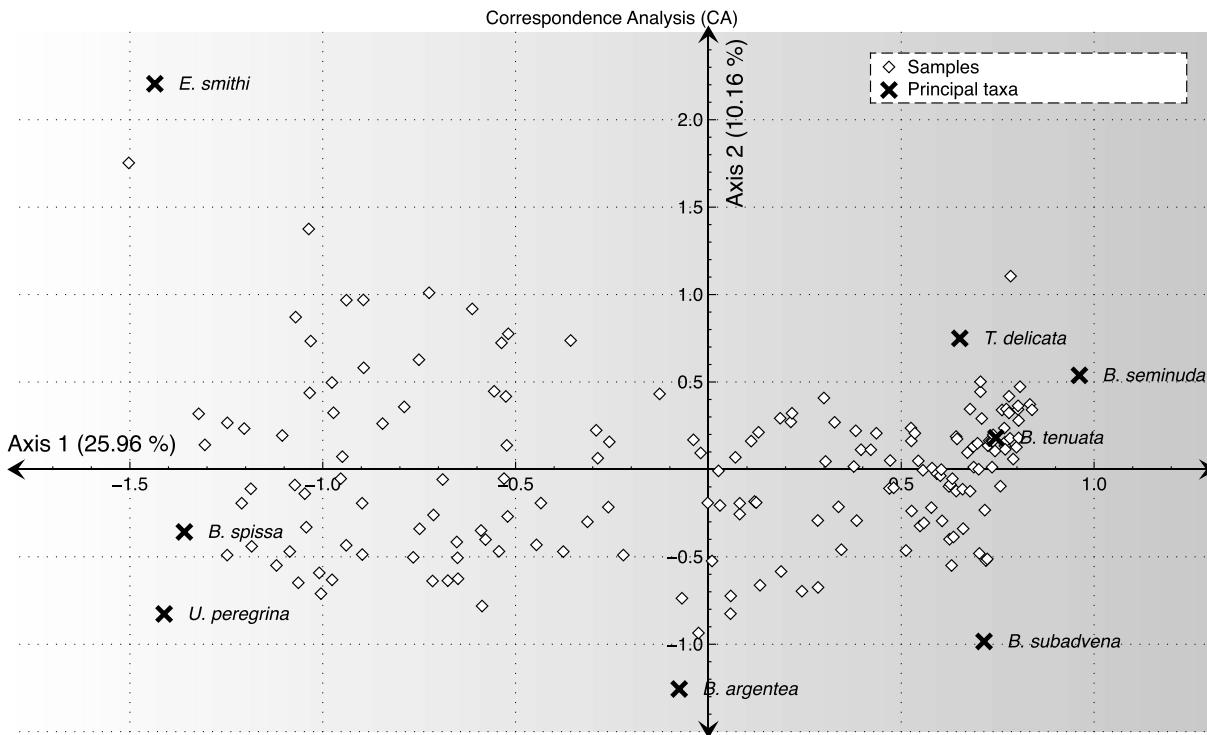


Figure 3. Biplot of the correspondence analysis based on the species abundance data set, roughly covering the last 80,000 years. The first and second axes account for 25.96% and 10.16% of the total variation, respectively. Both samples and principal taxa are plotted on the graph.

groups are well separated along the first axis. *Bolivina seminuda* (constituting from 1 to 54% of the assemblage), *B. subadvena* (0–63%), *T. delicata* (1–33%), and *B. tenuata* (2–60%) are grouped together within score values ranging from ~0.6 to ~1.0 along the first axis and will be referred to hereafter as the *seminuda* assemblage. *Uvigerina peregrina* (4–49%), *B. spissa* (8–43%), *E. smithi* (0–40%), and *B. argentea* (0–48%) are distributed between ~–1.4 and ~–0.1 and will be referred to as *peregrina* assemblage. This grouping is consistent with the downcore distribution of these species (Figure S3). The CA also shows that samples are well divided into two main groups (Figure 3), corresponding to samples dominated either by the *seminuda* assemblage or by the *peregrina* assemblage. A third group of samples corresponds to samples where the contribution of *seminuda* and *peregrina* assemblages is lower. These samples are dominated by a foraminiferal assemblage containing all other species and referred hereafter as the others fauna.

The first axis CA scores match well with the NGRIP $\delta^{18}\text{O}$ record [Johnsen et al., 2001] (Figure S4) and show positive excursions during interstadials and negative values during stadials. The pattern shown on the second axis differs significantly from the NGRIP $\delta^{18}\text{O}$ record (Figure S4). Main positive excursions are recorded in the transition between the Younger Dryas and the Holocene, during the Heinrich (H) events 2 to 6, and before the DO4, and between DO14 and 15, DO18 and 19, and DO19 and 20. Negative excursions occurred during the Holocene, DO3, and DO9, and in between DO13 and 14, DO18 and 19, and DO19 and 20.

3.3. Downcore Record of Faunal Assemblages and Descriptors

3.3.1. Overall Trends

The variations observed in the *seminuda* assemblage record, as well as for each species taken individually (Figure 2 and Figure S3), follow a trend similar in shape and intensity to the NGRIP oxygen isotope [Johnsen et al., 2001] record. Foraminiferal species assigned to the *seminuda* assemblage dominate samples (Figure S3) during the Holocene and the Bølling-Ållerød, and all DO interstadials during the MIS 2, 3, 4, and 5a. By contrast, the *peregrina* assemblage dominates during the Younger Dryas, the Last Glacial Maximum (LGM), and cold stadials, including stadials corresponding to Heinrich events (Figure 2 and Figure S3). The first CA axis is largely comparable with the *seminuda* and *peregrina* assemblage records and is likely to be

controlled variations in their relative abundances. The others assemblage, composed of all other (88) species, shows positive excursions during cold stadials, such as H2, H3, H4, H5, and H6, and the periods between DO11 and DO12, and DO18 and DO19. Negative excursions occurred during the Holocene, DO2, DO3, DO8, DO9, DO14, DO18, and DO19 and between DO18 and 19 and DO19 and 20 (Figure 2). Variance in the population of the others assemblage is similar to the variance of the second CA axis and thus is likely represented by this axis (Figure S4).

Several trends are noticeable in the distribution of the various faunal parameters as well. Diversity changes, as expressed by the Shannon index, show that the lowest diversity occurred during the Holocene, DO8, DO11, DO14, DO19, and DO20. The highest diversity was recorded during the Younger Dryas, H1, H2, H3, H4, H5, and H6 and in between DO11 and DO12 and DO18 and DO19. With regard to amplitude, it should be noted that the Shannon index exhibits a similar trend to the Mo/Al ratio overall (Figure 2). This diversity pattern is in good agreement with the others assemblage record previously described, a predictable result considering that rare species are supposed to lead biodiversity. The BFN is similar to the diversity indices and the Mo/Al and Cd/Al ratios. It shows a high abundance of benthic foraminifera during the Holocene, DO8, DO12, DO13, DO14, DO16, and DO19. Very low values (less than 100 ind g⁻¹) occurred during H3, H4, and H5.

3.3.2. DO18 Record

Foraminiferal trends were investigated at a higher resolution between ca 65.5 ka and 63 ka, during the interval corresponding to DO18 (Figures 4a and 4b). A ~500 years shift between assemblages and the NGRIP $\delta^{18}\text{O}$ record can be observed in this event, and possibly in a few more events, but is attributed to resolution artifacts and possible inconsistencies between age models. The *seminuda* assemblage was most abundant from ~65.4 to ~64.6 ka, when the NGRIP $\delta^{18}\text{O}$ record [Johnsen *et al.*, 2001] reached its highest values. The *peregrina* assemblage dominated from ~64.6 to ~63.6 ka, when $\delta^{18}\text{O}$ values were intermediate, between the DO18 maximum and the following H6. Finally, the others assemblage was most abundant around ~63.6 ka, during the H6, when the $\delta^{18}\text{O}$ values were the lowest. The Shannon index and the Mo/Al and Cd/Al ratios exhibit the same pattern overall. The Shannon index indicates a low diversity and high dominance during the first part of the event, then an intermediate diversity and dominance during the second part of the event, and a high diversity and low dominance during the last part of the event (Figure 4a). The Mo/Al and Cd/Al ratios were higher when the diversity was the lowest during the first part of the DO18 and progressively increase until the end of the event. The BFN was only high at ~65.1 ka, at the top of the DO18, when the Mo/Al ratio was the highest during the interval dominated by the *seminuda* assemblage but was relatively low in every other sample.

3.4. Towards an Oxygen Reconstruction

We compile known ecological preferences of species that compose three assemblages from the literature (Table 1; for more details, refer to the Text S1). It can thus be assumed that the *seminuda*, *peregrina*, and others assemblages are indicators of dysoxic, suboxic, and oxic conditions, respectively (in the sense of Moffitt *et al.* [2014, 2015a]; 0.1–0.5 mL.L⁻¹, 0.5–1.4 mL.L⁻¹, and > 1.4 mL.L⁻¹) and that the first CA axis corresponds to oxygenation.

The temporal variation of the dysoxic *seminuda* and suboxic *peregrina* assemblages are 180° out of phase (Figure 2). Occasional small deviations in this relationship correspond to variations in relative abundance of the oxic others assemblage (Figures 2 and 4a). These dysoxic and suboxic assemblages appear intimately related to the NGRIP $\delta^{18}\text{O}$ record of Johnsen *et al.* [2001] as all three records exhibit an almost identical variability (Figure 2). Indeed, global warming and cooling events recorded in the NGRIP likely affected export production and ventilation in water masses along the northeast American Coast [Hendy and Kennett, 2003; Crusius *et al.*, 2004; Cartapanis *et al.*, 2011]. This means that species who survive in these rapidly changing and unstable conditions (i.e., species from the dysoxic and suboxic assemblages) are the best adapted ones, as they are able to react quickly [Cannariato *et al.*, 1999]. The dysoxic *seminuda* assemblage thus dominated samples during warm interstadials (DO events), while the oxic others assemblage was abundant during intervals corresponding to H events (Figure 2). The suboxic *peregrina* assemblage was more abundant during regular stadials, when [O₂] was intermediate. These variations in dominance of the dysoxic, suboxic, and oxic assemblages correspond to geographical shifts of opportunistic species in response to extension or contraction of the OMC [Cannariato *et al.*, 1999].

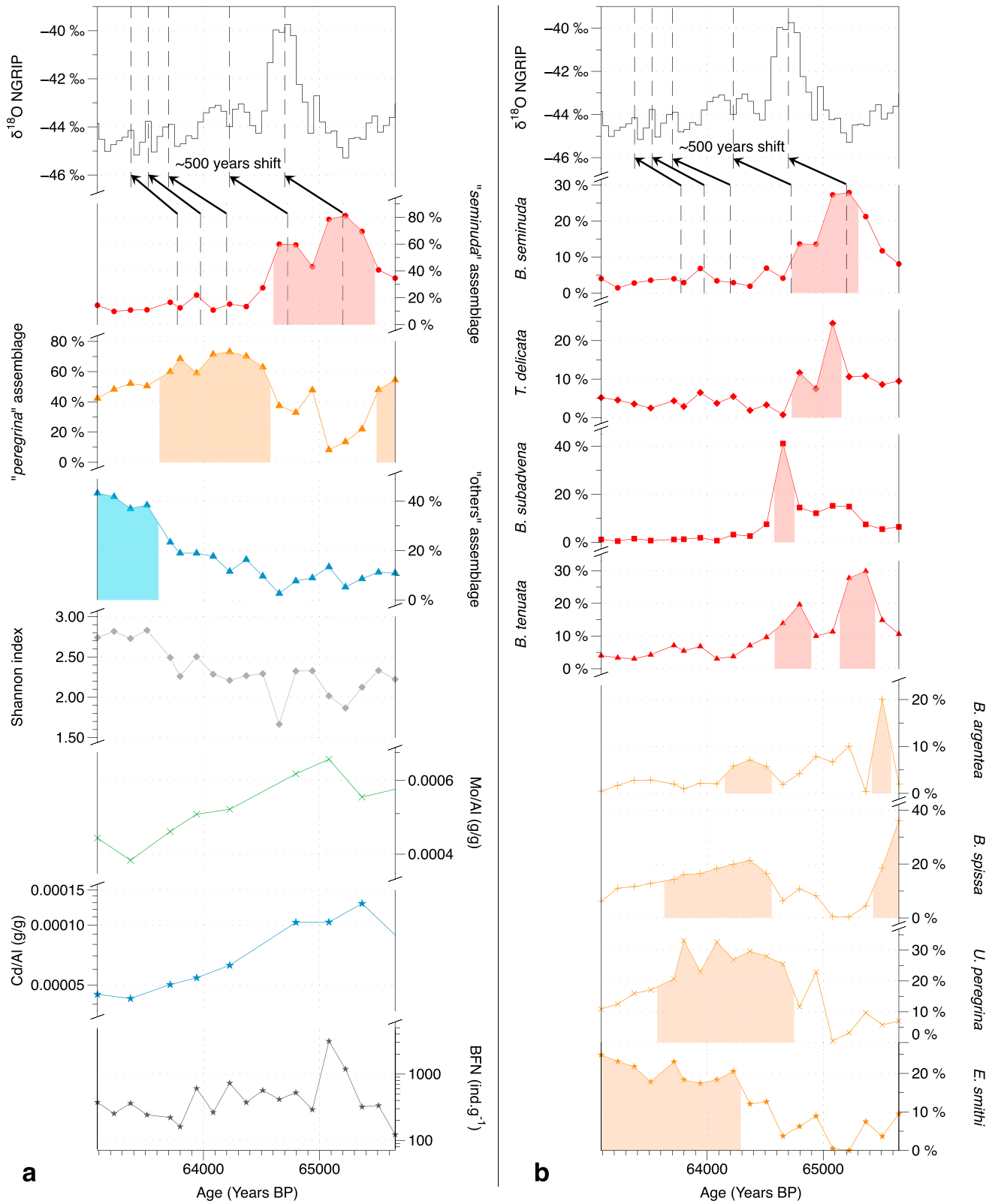


Figure 4. (a) Isotopic composition of the NGRIP ice core [Johnsen *et al.*, 2001] during the DO18 event, showing the relative abundance of the *seminuda*, *peregrina*, and others assemblages; the Shannon index reflecting diversity changes; the Mo/Al and Cd/Al ratios from Cartapanis *et al.* [2011, 2014]; and the normalized Benthic Foraminiferal Number (BFN: ind.g^{-1}), reflecting the absolute abundance of taxa. (b) Isotopic composition of the NGRIP ice core [Johnsen *et al.*, 2001] during the DO18 event, showing the faunal succession of the taxa composing the *seminuda* and *peregrina* assemblages. Colored areas correspond to maximum abundance of species.

Table 1. Oxygen Content (mL.L^{-1}) Reported in the Literature for Species From the *seminuda*, *peregrina*, and Others Assemblages^a

	$[\text{O}_2]$ Gradient (mL.L^{-1})	References
<i>Bolivina seminuda</i>	0.1–0.5	[1, 2]
<i>Bolivina subadvena</i>	0.1–0.5	[1]
<i>Takayagania delicata</i>	0.1–0.5	[1]
<i>Bulimina tenuata</i>	0.1–0.5	[1, 3]
<i>Bolivina argentea</i>	0.5–1.4	[3, 4]
<i>Uvigerina peregrina</i>	0.5–1.4	[3, 4]
<i>Bolivina spissa</i>	0.5–1.4	[1, 3, 4]
<i>Epistominella smithi</i>	0.5–1.4	[1, 3]
Other species	>1.4	[2, 4]

^a1, *Sen Gupta and Machain-Castillo* [1993] (average value between localities reported in the paper); 2, *Kaiho* [1994, 1999]; 3, *Cannariato and Kennett* [1999, and references therein]; and 4, *Moffitt et al.* [2014, 2015a, and references therein].

By using their respective relative abundance in the dysoxic, suboxic, and oxic assemblages, each sample was plotted on a ternary diagram (Figure 5). Samples are mainly distributed along the dysoxic-suboxic axis, with some further variation along the suboxic-oxic axis, and little along the dysoxic-oxic axis (Figure 5). As a result, each sample can be projected on an estimated $[\text{O}_2]$ curve. From 100% to 20% dysoxic assemblage relative abundance, samples are projected horizontally onto the first part of the $[\text{O}_2]$ curve to give the estimate. When the relative abundance of the dysoxic assemblage becomes low (less than 20%), and the oxic assemblage starts to develop, samples are projected vertically on the second part of the curve to give the estimate (Figure 5). The cutoff value was defined as 20%, as below this value the dysoxic assemblage is relatively stable over time under suboxic and oxic conditions (where only the suboxic and oxic assemblages vary in abundance; Figure 4a). Three dissolved oxygen values are assigned: 0.1 mL.L^{-1} for maximum abundance of the dysoxic assemblage, 0.5 mL.L^{-1} for the transition between the dysoxic and suboxic assemblages, and 1.4 mL.L^{-1} for the transition between the suboxic and oxic assemblages, on the basis of species ecological preferences reported in the literature [i.e., *Sen Gupta and Machain-Castillo*, 1993; *Kaiho*, 1994; *Cannariato and Kennett*, 1999] and recent estimates [*Moffitt et al.*, 2015a, and references therein]. According to the detailed assemblage changes investigated for DO18 (Figure 4a), the transition between dysoxic and suboxic dominated samples was set at ~50% of each assemblage. The transition between the suboxic and oxic samples was set at ~50% of suboxic and ~30% of oxic assemblage (Figure 4a). For each sample, an

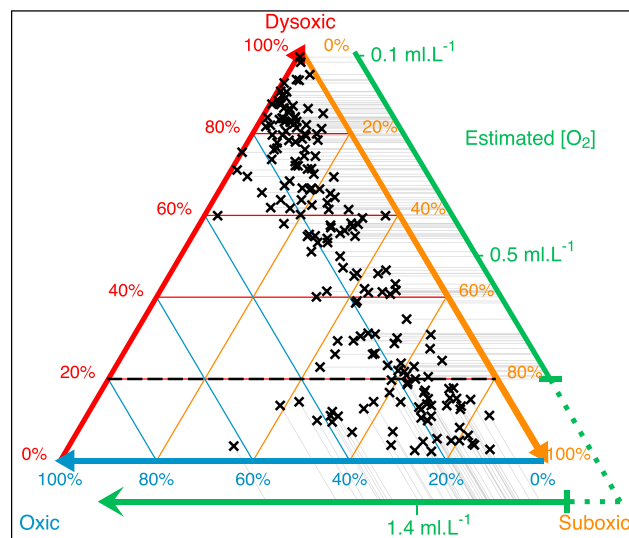


Figure 5. Ternary diagram plotting the relative abundance of the dysoxic *seminuda*, suboxic *peregrina*, and oxic others assemblages for each sample. Above the dashed line, points are projected horizontally onto the green line to give an estimation of $[\text{O}_2]$. Below the line, points are projected vertically to give an estimate.

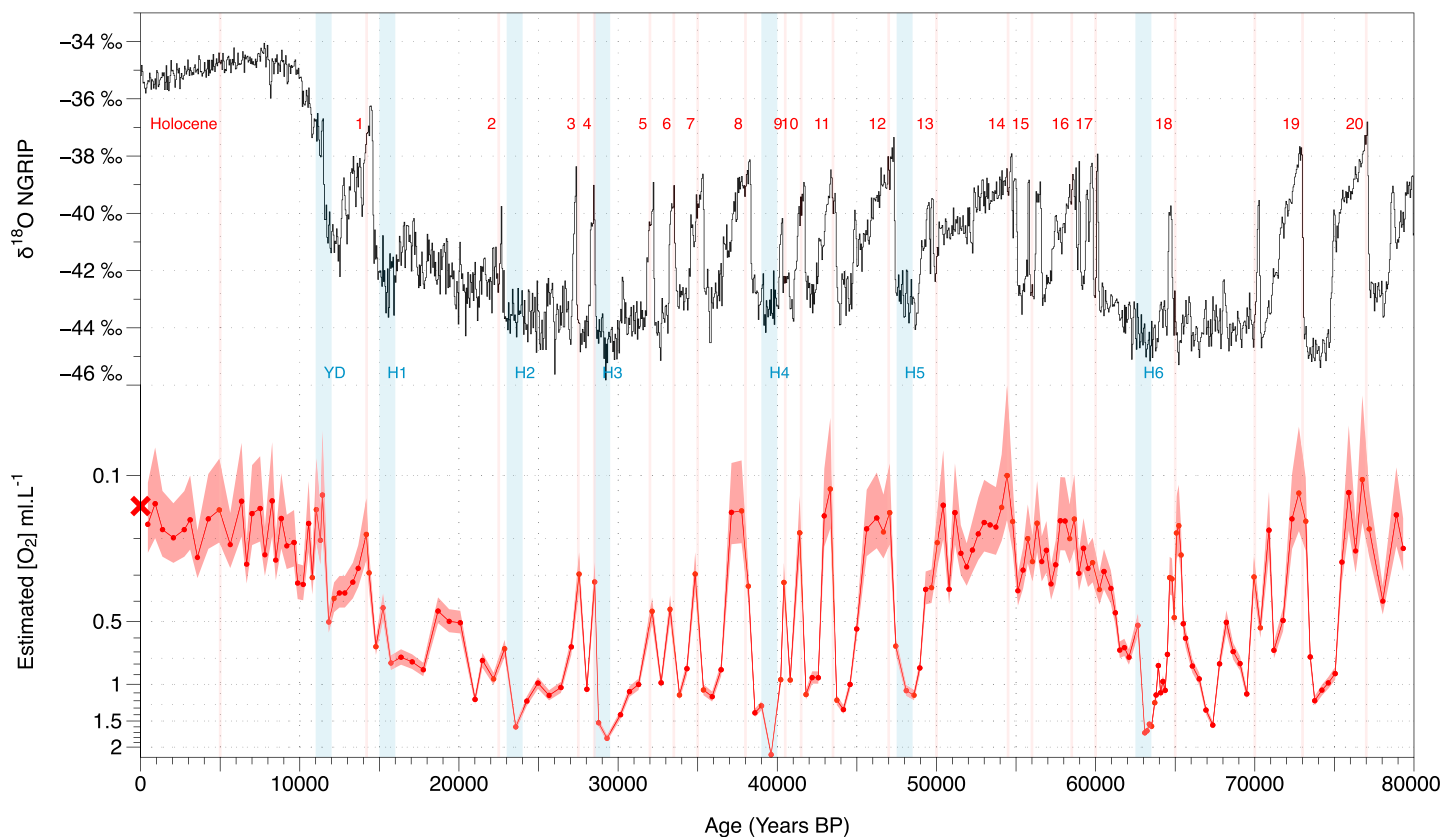


Figure 6. Isotopic composition of the NGRIP ice core [Johnsen *et al.*, 2001], showing the estimated [O₂] curve (mL.L⁻¹). The red cross (0.13 mL.L⁻¹) corresponds to modern [O₂] from the World Ocean Atlas 2013 data set (<http://www.nodc.noaa.gov/OC5/wao13/>). The red area corresponds to the 95% confidence interval based on the standard deviation of [O₂] downcore.

estimation of oxygen value is then interpolated (Figure 6). This interpolation enables us to provide the first semiquantitative record of [O₂] for the last glacial in the northeastern Pacific.

4. Discussion

4.1. Oxygen History off Baja California During the Last 80 kyr

The estimated oxygenation signal (Figure 6) is similar to the δ¹⁸O record from Greenland [Johnsen *et al.*, 2001]. This provides further evidence of the already reported global climate connections between the northeast Pacific and high latitudes of the Northern Hemisphere, specifically, ocean productivity and ventilation changes recorded in ice cores. This estimate shows very low oxygen values (between ~0.1 and ~0.5 mL.L⁻¹) during interstadials, higher values during regular stadials (~1 mL.L⁻¹), and similar maximal values during stadials corresponding to Heinrich events in the Atlantic Ocean (~2 mL.L⁻¹). Thus, Core MD02-2508 mostly exhibits dysoxic and suboxic conditions with rare occurrences of the oxic conditions almost only associated with H events. Modern dissolved oxygen content at 600 m deep off Baja California averages 0.13 mL.L⁻¹ (from the Ocean Data View software [Schlitzer, 2017; <http://odv.awi.de>] and the World Ocean Atlas 2013 data set [Garcia *et al.*, 2014; <http://www.nodc.noaa.gov/OC5/wao13/>]), in good agreement with our modern estimate. This single calibration point takes into account the relative contribution of all faunal components and therefore corroborates the reliability of the approach (Figure 6) to semiquantitatively reconstruct bottom water dissolved oxygen changes in the area. It is worth noting that estimated [O₂] values increase up to 2 mL.L⁻¹ during some stadials corresponding to Heinrich events within the Atlantic Ocean, indicating a collapse of the OMZ during these periods, while DO events are characterized by dissolved oxygen level down to 0.1 mL.L⁻¹. Interestingly, the Holocene shows relatively low [O₂] values (similar to those recorded during DO events, which are between ~0.1 and ~0.5 mL.L⁻¹) in contrast with the δ¹⁸O record from Greenland,

which exhibits higher values during the Holocene than during warm interstadials (Figure 6). This phenomenon may suggest that the relationship between conditions in Greenland and the intermediate water off California is modulated and smoothed during warm conditions, preventing $[O_2]$ from reaching lower values during the Holocene.

Several studies based on benthic foraminifera have already been performed along the California Coast at sites Ocean Drilling Program-893A (ODP-893A), [Cannariato *et al.*, 1999], ODP-1017E [Cannariato and Kennett, 1999], MVO811-15JV, MD02-2503, and MD02-2504 [Ohkushi *et al.*, 2013; Moffitt *et al.*, 2014]. Our new MD02-2508 record is located southward of these and thus significantly extends the latitudinal range of northeast Pacific margin foraminiferal records (Figures 1 and 7). Core MD02-2508 is dominated by a dysoxic assemblage during interstadials and a suboxic assemblage during stadials (Figure 7), which is similar to other sites such as ODP-893A in the Santa Barbara basin [Cannariato *et al.*, 1999]. However, it differs in the relative contribution of these assemblages. The suboxic assemblage remains relatively rare at ODP site 893A, and instead exhibits a dominating oxic fauna, in contrast to the present study. The Santa Barbara Basin can exhibit highly depleted dissolved oxygen concentrations due to its geographic configuration (closed basin). This trend is reinforced in the open ocean ODP site 1017E, where the suboxic and oxic assemblages are largely dominating [Cannariato and Kennett, 1999] while the dysoxic assemblage is relatively rare (Figure 7). These differences between sites are related to their location with regard to the OMZ. ODP site 1017E is the farthest north (Point Concepción), at a more distal position from the OMZ core than site MD02-2508, thus experiencing more oxygenated conditions all year long. According to Helly and Levin [2004, Figure 2], the depth interval where $O_2 < 0.5 \text{ mL.L}^{-1}$ is between 500 and 700 m deep at 34°N , in contrast to 100 to 1000 m deep off Baja California. The $< 0.2 \text{ mL.L}^{-1}$ layer is almost absent at 34°N but extends from 200 to 800 m off Baja California, which is in good agreement with our $[O_2]$ estimate (Figure 6).

Ohkushi *et al.* [2013] also investigated faunal variations in SBB at a depth of 481 and 569 m. The relative abundance of the dysoxic, suboxic, and oxic assemblages at this site are in between those at ODP sites 893A and 1017E [see Ohkushi *et al.*, 2013, Figure 3]. The record indicates slightly more oxygenated conditions, as the suboxic and dysoxic assemblages were more abundant during the Holocene than site MD02-2508, which was largely composed of the dysoxic assemblage. Moffitt *et al.* [2014] add another core sampled near Point Concepción to the SBB collection but located in shallower waters and at a more distal position to the shore than Ohkushi *et al.* [2013]. As expected, this core shows an abundant suboxic assemblage during the Holocene and Bølling/Allerød while the oxic (that is, weak hypoxic) dominates during the Younger Dryas and the LGM. Santa Barbara Basin and Point Concepción records often display an abundant and dominating oxic assemblage potentially associated with the disappearance of OMZ conditions at these latitudes (Figure 7).

4.2. Export Production Impact on Oxygenation

For several decades, many studies have disagreed on the relative importance of export production and ventilation to the oxygenation balance of water masses [Herguera *et al.*, 2010]. Some propose that changes in biological production are principally responsible for the oxygen variability within the ENP OMZ [Phleger and Soutar, 1973; Crusius *et al.*, 2004; Ortiz *et al.*, 2004; Murdmaa *et al.*, 2010; Praetorius *et al.*, 2015]. The BFN calculated in this study is likely to mirror export production [Herguera and Berger, 1991; Herguera, 1992]. Naidu and Malmgren [1995] and Den Dulk *et al.* [2000] considered the BFN to be unreliable in OMZ areas as it is known to be limited by two opposing factors: (1) Unfilled respiration requirements in conditions (almost) depleted in oxygen and (2) competition and predation pressure leading to the absence of a single dominating taxa [Phleger and Soutar, 1973; Bernhard and Reimers, 1991]. The latter is, however, difficult to evidence and much more problematic to quantify. We are thus fully aware that for low $[O_2]$ environments, one should be cautious in the interpretation of the BFN as a productivity indicator, for the reasons quoted above. However, the comparison of the BFN with other productivity tracers investigated in Core MD02-2508 by Cartapanis *et al.* [2011, 2014] still allows us to limit biases and gain reliable insights into productivity changes off Baja California. The BFN record correlates well to PC1 from Cartapanis *et al.* [2011] and to the Cd/Al record of Cartapanis *et al.* [2011, 2014], which are interpreted as export production tracers [Nameroff *et al.*, 2002; Dean *et al.*, 2006; Tribovillard *et al.*, 2006; Van der Weijden *et al.*, 2006] as they show an increase (decrease) in benthic foraminiferal abundance associated with a higher (lower) export production during interstadials (stadials; Figure 2). Cadmium is considered a “nutrient-like” element concentrated by

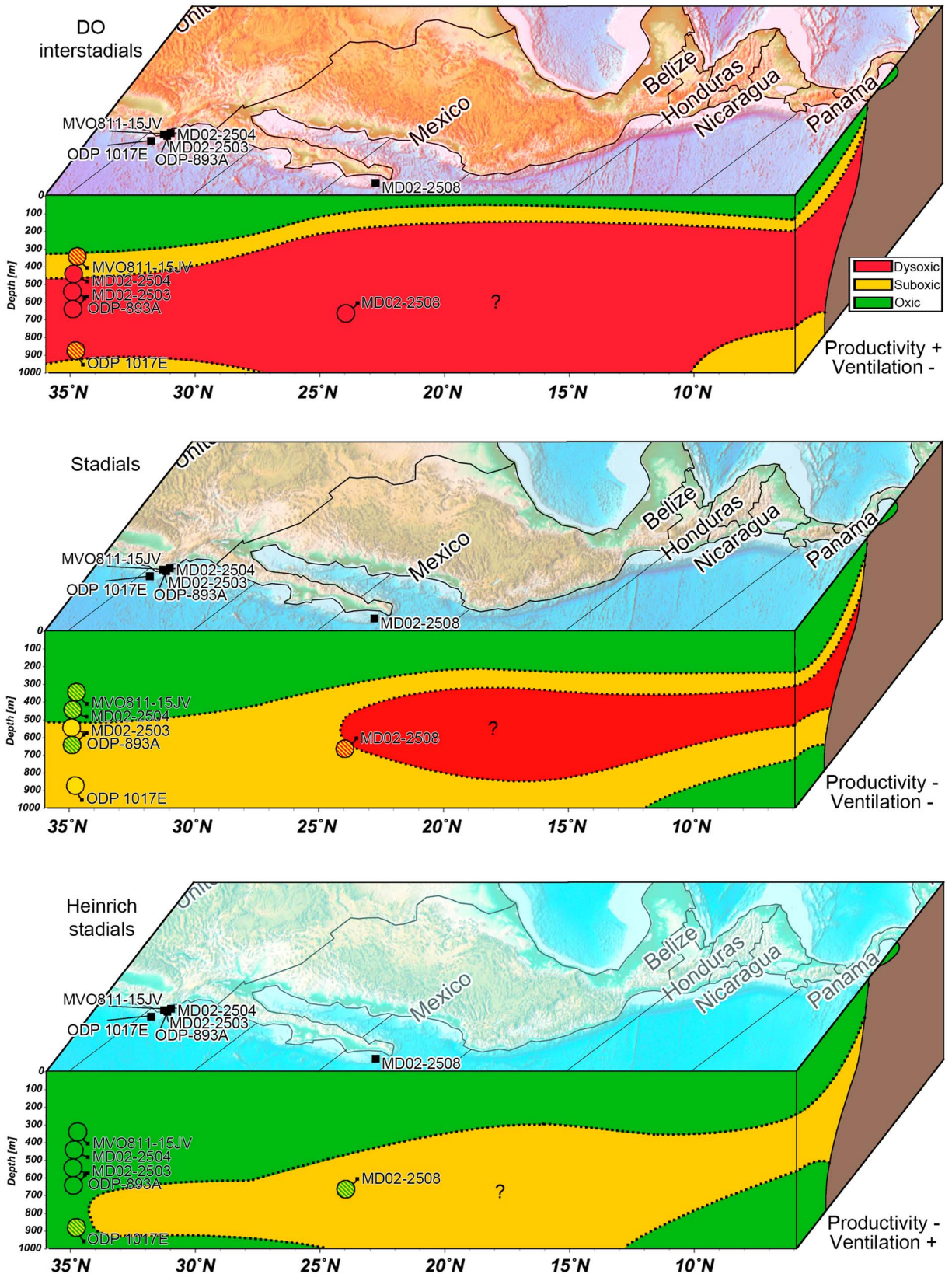


Figure 7. Schematic of ENP OMZ extension during interstadials, stadials, and Heinrich stadials, based on benthic foraminifera studies [Cannariato and Kennett, 1999; Cannariato et al., 1999; Ohkushi et al., 2013; Moffitt et al., 2014, 2015b].

plankton, delivered to the sediment along with organic and other marine particles. Its concentration depends on the export production, and it is retained in the sediment if dissolved oxygen concentration is low enough [Tribouillard *et al.*, 2006]. This BFN also shows similarities with the estimated downcore $[O_2]$ record during stadials and interstadials. On the whole, the export production signal increases (decreases) with a fall (rise) of the $[O_2]$ during warm interstadials (cold stadials) suggesting an inverse relationship between each during these intervals [Herguera *et al.*, 2010, and references therein]. Export production is reported to play a key role in the oxygenation in the area [Ortiz *et al.*, 2004; Cartapanis *et al.*, 2011] by consuming oxygen during the remineralisation of organic matter (the higher the export production, the higher the degradation of the organic matter, the lower the resulting $[O_2]$). This phenomenon is well visible for the more finely sampled DO18 period (Figure 4b), where the BFN increased during the warmer interstadial maximum, then decreased with the subsequent cooling.

The high similarity between the semiquantitative record of $[O_2]$ and the NGRIP $\delta^{18}O$ record [Johnsen *et al.*, 2001] suggests the influence of a global scale mechanism on oxygen variability in the OMZ [Herguera *et al.*, 2010], such as the oceanic circulation [Behl and Kennett, 1996; Cannariato *et al.*, 1999; Zheng *et al.*, 2000; Karstensen *et al.*, 2008]. However, through a succession of related mechanisms, global climate changes might be influencing oxygenation via regional parameters such as the amount of water mass transported from the far north Pacific [van Geen *et al.*, 2006] and export productivity [Ortiz *et al.*, 2004; Cartapanis *et al.*, 2011]. The atmospheric connection between the high latitudes of the Atlantic Ocean and the northeast Pacific are still poorly known [Zheng *et al.*, 2000; Schmittner *et al.*, 2007] but several hypotheses proposed a few years ago are still relevant for explaining an enhanced (reduced) export productivity recorded during warm (cold) intervals in Greenland [Schmittner *et al.*, 2007]. A weakening of southward winds off coasts in the northeastern Pacific during cold intervals that lowers wind-driven upwelling activity and export production, has been proposed to explain the connection between the north Atlantic temperatures and ENP oxygenation [Cartapanis *et al.*, 2011, and references therein; Schmittner *et al.*, 2007]. As the BFN does not perfectly match the $[O_2]$ signal, another parameter is likely affecting the variation in oxygen concentration of water masses within the northeastern Pacific Ocean.

4.3. Implications of Enhanced Ventilation

Because of the imperfect match, export production was reported as being not the only mechanism responsible for $[O_2]$ variability, as it can be significantly influenced by oceanic circulation [Schmittner *et al.*, 2007; Karstensen *et al.*, 2008]. On the other hand, recent studies have also mentioned that organic carbon burial rates near Baja California seem to vary independently as they can be biased by preservation, which also depends on oxygenation [Nederbragt *et al.*, 2008]. Moreover, since not every low export production value in our data is associated with oxygen-rich conditions (up to $\sim 2 \text{ mL L}^{-1}$), export production alone cannot be responsible for the O_2 pulses experienced during stadials associated with Heinrich events. Mudd *et al.* [2010] suggested that MIS 1 and 5 were associated with high primary production, while MIS 2–4 show lower values with some high-production events associated with DO events. Indeed, even though the estimated $[O_2]$ signal is relatively similar to the records provided by export production tracers, some differences remain in several interstadials (e.g., DO2–DO7) in which the $[O_2]$ record closely follows the DO event signal but export production tracers do not show any variation. This could result from these tracers not well reflecting changes during the events or if export production is not changing during events where $[O_2]$ is changing. If the latter is correct, then ventilation should also be regarded as a key factor that could be responsible for $[O_2]$ variations recorded downcore [Behl and Kennett, 1996; Cannariato *et al.*, 1999; Nederbragt *et al.*, 2008; Schmittner *et al.*, 2007; van Geen *et al.*, 2006; Zheng *et al.*, 2000; Karstensen *et al.*, 2008]. The variation along the second CA axis is highly similar to the relative abundance of the oxic others assemblage (Figure S4). The main positive excursions on this axis, as well as peaks in abundance of oxic species, occur during H events. This pattern is also similar to the serial/spiral benthic foraminiferal test ratio already reported as an indicator of the redox state of the sediments and is influenced by the bottom water ventilation and current velocity [Nameroff *et al.*, 2002; Murray, 2006; Schumacher *et al.*, 2007; Ovsepyan and Ivanova, 2009]. Spiral (planispiral and trochospiral) forms are usually considered as epibenthic (surface dwellers) while the serial forms are likely to live within the sediments (shallow to deep infaunal) [Corliss, 1991]. As the sediment becomes depleted in oxygen, the endofaunal species tend to migrate to the sediment/water interface, leading to an increase in the serial/spiral forms ratio [Jorissen *et al.*, 1995, 2007]. In addition, this oxic fauna is dominated

by *Cibicidoides*-like species during Heinrich events, which are known to react to bottom water ventilation enhancement [Murdmaa et al., 2010].

According to Menviel et al. [2014] and Timmermann et al. [2005], oceanic circulation was enhanced in the Pacific realm during Heinrich intervals, particularly during the H4 (largest of the first six H events, maximum at ~39.5 ka, in agreement with the results) which is associated with a strong cooling over Greenland and the North Atlantic [Hemming, 2004; Herguera et al., 2010; Menviel et al., 2014]. The formation and transport of deep bottom currents such as the North Pacific Deep Water and Antarctic Bottom Water were enhanced by a salinity increase in the surface water of the Pacific Ocean [Rodriguez-Sanz et al., 2013], through atmospheric connections with the Atlantic Ocean, and through a reduced Atlantic Meridional Overturning Circulation (AMOC) during stadials, with the largest reductions occurring during Heinrich events, particularly H4 [Henry et al., 2016], which is associated with large IRD events. This led to greater ventilation of intermediate and deep bottom waters (down to 2000 m) in the North Pacific Ocean and weaker upwelling in the eastern Pacific basin [Menviel et al., 2012, 2014; Chikamoto et al., 2012], resulting in higher oxygenation [Zheng et al., 2000; van Geen et al., 2006; Schmittner et al., 2007]. These periods of potentially enhanced ventilation that occur during Heinrich stadials also exhibit relatively low BFN and Cd/Al ratio values (Figure 4a) suggesting a low export production. This suggests that both parameters play an important role in the resulting oxygenation [Dean et al., 2006] and reinforces the hypothesis that both are intrinsically linked [van Geen et al., 2006] as oceanic circulation can not only directly affect oxygenation but also export productivity and the intensity of upwellings, which in turn also impact [O₂] [Herguera et al., 2010; Schmittner et al., 2007].

4.4. Paleoeological Implication of Assemblages

Investigation of DO18 at higher resolution allows us to identify an ecological succession of the three assemblages during a period of decrease followed by increase in dissolved oxygen concentration in bottom waters. Each assemblage became more abundant according to their preference for O₂ (Figures 2, 4a, and 6). With increasing oxygen, a gradual shift from suboxic to dysoxic conditions followed by a shift from dysoxic to suboxic and finally oxic conditions can be observed. This succession is visible in almost every interstadial/stadial transition of the record, until MIS 5a. Inconsistencies in the succession are attributed to sampling resolution issues and the time needed for the oxic assemblage to settle. The focus on the DO18 event shows that moving from dysoxic to oxic conditions the populations of *B. seminuda*, *T. delicata*, and *B. subadvena*; *B. tenuata*; *B. argentea*; *B. spissa*; *U. peregrina*; and *E. smithi* rise and fall in succession (Figure 4b), in good agreement with their preferences for O₂ and the oxygen gradient. No consistent sequence could be distinguished for other DO events due to issues with the lower resolution used outside of DO18. Interestingly, even though the three assemblages show a symmetric distribution between the beginning and the end of the dysoxic event (Figure 4a), the succession of species within these assemblages is asymmetric [Cannariato et al., 1999]. Thus, *B. tenuata* and *B. spissa*/*B. argentea* are more abundant at the beginning of the DO18, while *B. subadvena* and *U. peregrina*, respectively, dominate the dysoxic and suboxic assemblages at the end of the event. This suggests that other ecological parameters, such as differences in export productivity visible in the DO18 data or diversity leading to competition (Figure 4a), or differences in timing and speed of environmental changes, as DO are supposed to show a rapid warming followed by a longer cooling, might be responsible for the difference in the presence or absence of species for equivalent oxygen conditions before and after the DO event.

Low oxygenated waters are associated with very specific benthic foraminifera capable of living in such a stressful environment and thus can lead to low diversity and high dominance of these taxa [Sen Gupta and Machain-Castillo, 1993]. More oxygenated waters induce favorable conditions for most species and lead to a higher diversity with more competition and lower dominance [Levin et al., 1991, 2000; Den Dulk et al., 1998]. As a consequence, diversity indices have frequently been used as indicators of past oxygenation [Van der Zwaan et al., 1999; summarized in Murray, 2006; Jorissen et al., 2007]. The Shannon index is comparable with the Mo/Al ratio measured by Cartapanis et al. [2011, 2014], which is interpreted as a proxy for dissolved oxygen (broad increase during MIS 2 and MIS 3). Molybdenum is referred to as a "conservative element". Its concentration is uniform at all depths throughout the different oceans and it precipitates under oxygen-deficient conditions, reflecting the redox state of its environment [Nameroff et al., 2002; Tribouillard et al., 2006; Scholz et al., 2014]. However, the Mo/Al ratio is subject to a threshold effect (e.g., precipitation for Molybdenum starts when O₂ < ~0.2 mL L⁻¹ [Cartapanis et al., 2011; Moffitt et al., 2015a]) and can be

affected by dilution with terrigenous inputs during accumulation [Blanchet *et al.*, 2007]. Moreover, the behavior of this trace metal element is likely to be affected by changing redox conditions during diagenesis, leading to its remobilization [Tribovillard *et al.*, 2006]. The Shannon index is also similar to the oxic assemblage reflecting the abundance of oxic taxa and thus an increase in diversity being associated with an increase in the number of oxic species, which is expected. This relationship indicates that the transition from dysoxic to suboxic conditions has little impact on diversity. However, both signals are somewhat different from our estimated $[O_2]$ record. Gooday [2003] suggests that during oxic conditions (when $[O_2]$ is not limiting anymore) diversity is likely responding to increased production. Van der Zwaan *et al.* [1999] also suggest that the presence or absence of taxa depends on oxygen concentration whereas their abundance or dominance likely depends on the amount of organic matter and affects diversity when $[O_2]$ is not limiting. The diversity indices might thus be subject to a threshold effect and display an intertwined signal, where they reflect $[O_2]$ within a certain range, after which they are largely affected by export production. Differences observed between diversity indices and oxygenation and productivity records are therefore consistent.

5. Conclusions

In this study, we investigated past variations of benthic foraminiferal assemblages in Core MD02-2508 to produce a semiquantitative O_2 record of the ENP OMZ over the last 80 kyr. Three assemblages reflecting dysoxic, suboxic, and oxic conditions were identified using correspondence analysis. These were analyzed to obtain the first reconstruction of estimated $[O_2]$ for the northeastern Pacific. This oxygenation signal is very similar to the NGRIP $\delta^{18}O$ record, which implies a tight correlation between global climate and oxygenation; that is, dysoxic conditions during interstadials, suboxic during stadials, and oxic during Heinrich-event stadials.

Both the serial/spiral test ratio and the oxic assemblage record show similar signals, with remarkable excursions that suggest enhanced oxygenation during stadials corresponding to Heinrich events. These O_2 pulses can be attributed to enhanced ventilation within the Northeast Pacific region during Heinrich stadials as suggested by modeling-based oceanic circulation reconstructions. However, it does not exclude that ventilation might have played a significant role on oxygenation during other stadials and interstadials. Export production was also investigated by focusing on two independent tracers, micropaleontological (benthic foraminiferal abundance), and geochemical (Cd/Al ratio), due to its high similarity with the estimated downcore $[O_2]$ reconstruction. Indeed, high (low) export production correlates well with low (high) oxygenation suggesting this process should also be regarded as a key factor for $[O_2]$.

Geochemical signals recorded for Core MD02-2508 (e.g., Cd/Al and Mo/Al ratios [Cartapanis *et al.*, 2011, 2014]) failed to reflect several DO events for the last 80 kyr. However, these events were successfully recovered in the downcore oxygenation signal estimated using benthic foraminifera. This reinforces the common assumption that biological tracers have a high reliability for paleo-oxygenation studies, suggesting that multiproxy approaches should be favored whenever possible [Praetorius *et al.*, 2015].

Acknowledgments

Thanks to Noelle Buchet for the pre-processing of Core MD02-2508 and to Olivier Cartapanis for sharing his geochemical data from this core. Thanks also to Guillaume Leduc for discussion and advice regarding this study. Many thanks to Ross Marchant for proofreading and to the Editor and to the three reviewers for providing valuable suggestions improving the original manuscript. We thank the Agence Nationale de la Recherche for its financial support under projects ANR-12-BS06-0007 – CALHIS. Data are available in supporting information and will be stored in the PANGAEA data base (www.pangaea.de).

References

- Behl, R. J., and J. P. Kennett (1996), Brief interstadial events in the Santa Barbara basin, NE Pacific, during the past 60 kyr, *Nature*, 379, 243–246.
- Bernhard, J. M. (1992), Benthic foraminiferal distribution and biomass related to pore-water oxygen: Central California continental slope and rise, *Deep Sea Res. Part A*, 39, 586–605.
- Bernhard, J. M., and C. E. Reimers (1991), Benthic foraminifera population fluctuations related to anoxia: Santa Barbara Basin, *Biogeochemistry*, 15, 127–149.
- Blanchet, C. L., N. Thouveny, L. Vidal, G. Leduc, K. Tachikawa, E. Bard, and L. Beaufort (2007), Terrigenous input response to glacial/interglacial climatic variations over southern Baja California: A rock magnetic approach, *Quat. Sci. Rev.*, 26, 3118–3133.
- Buzas, M. A. (1990), Another look at confidence limits for species proportions, *J. Paleontol.*, 64, 842–843.
- Cannariato, K. G., and J. P. Kennett (1999), Climatically related millennial-scale fluctuations in strength of California margin oxygen-minimum zone during the past 60 kyr, *Geology*, 27, 975–978.
- Cannariato, K. G., J. P. Kennett, and R. J. Behl (1999), Biotic response to late Quaternary rapid climate switches in Santa Barbara Basin: Ecological and evolutionary implications, *Geology*, 27, 63–66.
- Cartapanis, O., K. Tachikawa, and E. Bard (2011), Northeastern Pacific oxygen minimum zone variability over the past 70 kyr: Impact of biological production and oceanic ventilation, *Paleoceanography*, 26, PA4208, doi:10.1029/2011PA002126.
- Cartapanis, O., K. Tachikawa, O. E. Romero, and E. Bard (2014), Persistent millennial-scale link between Greenland climate and northern Pacific oxygen minimum zone under interglacial conditions, *Clim. Past*, 10, 405–418.
- Caulle, C., K. A. Koho, M. Mojtahid, G. J. Reichart, and F. J. Jorissen (2014), Live (Rose Bengal stained) foraminiferal faunas from the northern Arabian Sea: Faunal succession within and below the OMZ, *Biogeosciences*, 11, 1155–1175.
- Caulle, C., M. Mojtahid, A. J. Gooday, F. J. Jorissen, and H. Kitazato (2015), Living (Rose-Bengal-stained) benthic foraminiferal faunas along a strong bottom-water oxygen gradient on the Indian margin (Arabian Sea), *Biogeosciences*, 12, 5005–5019.

- Chikamoto, M. O., L. Menviel, A. Abe-Ouchi, R. Ohgaito, A. Timmermann, Y. Okazaki, N. Harada, A. Oka, and A. Mouchet (2012), Variability in North Pacific intermediate and deep water ventilation during Heinrich events in two coupled climate models, *Deep Sea Res., Part II*, 61–64, 114–126.
- Corliss, B. H. (1991), Morphology and microhabitat preferences of benthic Foraminifera from the northwest Atlantic Ocean, *Mar. Micropaleontol.*, 17, 195–236.
- Crusius, J., T. F. Pedersen, S. Kienast, L. Keigwin, and L. Labeyrie (2004), Influence of northwest Pacific productivity on North Pacific Intermediate Water oxygen concentrations during the Bølling-Allerød interval (14.7–12.9 ka), *Geology*, 32, 633–636.
- Cushman, J. A. (1911), A monograph of the foraminifera of the North Pacific Ocean: Part 2. Textulariidae, *Bull. U. S. Natl. Museum*, 71, 1–108.
- Cushman, J. A. (1923), The foraminifera of the Atlantic Ocean, Part 4, Lagenidae, *Bull. U. S. Natl. Museum*, 104, 1–228.
- Cushman, J. A. (1926), Some Pliocene bolivinas from California, *Contrib. Cushman Lab. Foraminiferal Res.*, 2, 40–46.
- Cushman, J. A. (1927), Recent foraminifera from off the West Coast of America, in *Bulletin of the Scripps Institution of Oceanography, Technical ser.*, vol. 1, pp. 119–188, Univ. of California Press, Berkeley, Calif.
- Dansgaard, W., S. J. Johnsen, and H. B. Clausen (1993), Evidence for general instability of past climate from a 250-kyr ice-core record, *Nature*, 364, 218–220.
- Dean, W. E., Y. Zheng, J. D. Ortiz, and A. van Geen (2006), Sediment Cd and Mo accumulation in the oxygen-minimum zone off western Baja California linked to global climate over the past 52 kyr, *Paleoceanography*, 21, PA4209, doi:10.1029/2005PA001239.
- Den Dulk, M., G. J. Reichart, G. M. Memon, E. M. P. Roelofs, W. J. Zachariasse, and G. J. Van der Zwaan (1998), Benthic foraminiferal response to variations in surface water productivity and oxygenation in the northern Arabian Sea, *Mar. Micropaleontol.*, 35, 43–66.
- Den Dulk, M., G. J. Reichart, S. van Heyst, W. J. Zachariasse, and G. J. Van der Zwaan (2000), Benthic Foraminifera as proxies of organic matter flux and bottom water oxygenation? A case history from the northern Arabian Sea, *Palaeogeogr. Palaeoclimatol. Palaeoecol.*, 161, 337–359.
- Diz, P., and S. Barker (2016), Approaches and constraints to the reconstruction of palaeoproductivity from Cape Basin abyssal benthic foraminifera (South Atlantic), *J. Micropaleontol.*, 35, 195–204.
- Durazo, R. (2015), Seasonality of the transitional region of the California Current System of Baja California, *J. Geophys. Res. Oceans*, 120, 1173–1196, doi:10.1002/2014JC010405.
- Durazo, R., and T. R. Baumgartner (2002), Evolution of oceanographic conditions off Baja California: 1997–1999, *Prog. Oceanogr.*, 54, 7–31.
- Eberwein, A. (2007), *Holocene and Last Glacial Maximum (Paleo-) Productivity off Morocco: Evidence From Benthic Foraminifera and Stable Carbon Isotopes = (Paläo-) Produktivität im Holozän und Letzten Glazialen Maximum vor Marokko Erschlossen aus Benthischen Foraminiferen und Stablen Kohlenstoffisotopen, Berichte zur Polar- und Meeresforschung (Reports on Polar and Marine Research)*, pp. 548, Alfred Wegener Institute for Polar and Marine Research, Bremerhaven.
- Fatela, F., and R. Taborda (2002), Confidence limits of species proportions in microfossil assemblages, *Mar. Micropaleontol.*, 45, 169–174.
- Fontanier, C., F. J. Jorissen, L. Licari, A. Alexandre, P. Anschutz, and P. Carbonel (2002), Live benthic foraminiferal faunas from the Bay of Biscay: Faunal density, composition, and microhabitats, *Deep Sea Res., Part I*, 49, 751–785.
- Garcia, H. E., R. A. Locarnini, T. P. Boyer, J. I. Antonov, O. K. Baranova, M. M. Zweng, J. R. Reagan, and D. R. Johnson (2014), World Ocean Atlas 2013, in *Dissolved Oxygen, Apparent Oxygen Utilization, and Oxygen Saturation, NOAA Atlas NESDIS 75*, vol. 3, edited by S. Levitus and A. Mishonov (Technical Ed.). [Available at <https://www.nodc.noaa.gov/OC5/woa13/pubwoa13.html>].
- Gooday, A. J. (2003), Benthic foraminifera (Protista) as tools in deep-water palaeoceanography: Environmental influences on faunal characteristics, *Adv. Mar. Biol.*, 46, 1–90.
- Gotelli, N. J., and A. Chao (2013), Measuring and estimating species richness, species diversity, and biotic similarity from sampling data, in *Encyclopedia of Biodiversity*, vol. 5, 2nd ed., edited by S. A. Levin, pp. 195–211, Academic Press, Waltham, Mass.
- Hammer, Ø. (2014), PAST, PAleontological STatistics, version 3.04, Reference Manual, p. 224. [Available at <http://folk.uio.no/ohammer/past/past3manual.pdf>].
- Hammer, Ø., D. A. T. Harper, and P. D. Ryan (2001), PAST: Paleontological Statistics software package for education and data analysis, *Palaeontol. Electron.*, 4, 9.
- Heinrich, H. (1988), Origin and consequences of cyclic ice rafting in the northeast Atlantic Ocean during the past 130,000 years, *Quat. Res.*, 29, 142–152.
- Helly, J. J., and L. A. Levin (2004), Global distribution of naturally occurring marine hypoxia on continental margins, *Deep Sea Res., Part I*, 51, 1159–1168.
- Hemming, S. R. (2004), Heinrich events: Massive late Pleistocene detritus layers of the North Atlantic and their global climate imprint, *Rev. Geophys.*, 42, RG1005, doi:10.1029/2003RG000128.
- Hendy, I. L., and J. P. Kennett (2000), Dansgaard-Oeschger cycles and the California Current System: Planktonic foraminiferal response to rapid climate change in Santa Barbara Basin, Ocean Drilling Program hole 893A, *Paleoceanography*, 15, 30–42, doi:10.1029/1999PA000413.
- Hendy, I. L., and J. P. Kennett (2003), Tropical forcing of North Pacific intermediate water distribution during Late Quaternary rapid climate change?, *Quat. Sci. Rev.*, 22, 673–689.
- Henry, L. G., J. F. McManus, W. B. Curry, N. L. Roberts, A. M. Piotrowski, and L. D. Keigwin (2016), North Atlantic ocean circulation and abrupt climate change during the last glaciation, *Science*, 353, 470–474.
- Herguera, J. C. (1992), Deep-sea benthic foraminifera and biogenic opal: Glacial to postglacial productivity changes in the western equatorial Pacific, *Mar. Micropaleontol.*, 18, 79–98.
- Herguera, J. C., and W. Berger (1991), Paleoproductivity from benthonic foraminifera abundance: Glacial to postglacial change in the west-equatorial Pacific, *Geology*, 19, 1173–1176.
- Herguera, J. C., T. Herbert, M. Kashgarian, and C. Charles (2010), Intermediate and deep water mass distribution in the Pacific during the Last Glacial Maximum inferred from oxygen and carbon stable isotopes, *Quat. Sci. Rev.*, 29, 1228–1245.
- Johnsen, S. J., D. Dahl-Jensen, N. Gundestrup, J. P. Steffensen, H. B. Clausen, H. Miller, V. Masson-Delmotte, A. E. Sveinbjörnsdottir, and J. White (2001), Oxygen isotope and palaeotemperature records from six Greenland ice-core stations: Camp Century, Dye-3, GRIP, GISP2, Renland and NorthGRIP, *J. Quat. Sci.*, 16, 299–307.
- Jorissen, F. J., H. C. De Stigter, and J. G. V. Widmark (1995), A conceptual model explaining benthic foraminiferal microhabitats, *Mar. Micropaleontol.*, 22, 3–15.
- Jorissen, F. J., C. Fontanier, and E. Thomas (2007), Paleocyanographical proxies based on deep-sea benthic foraminiferal assemblage characteristics, in *Proxies in Late Cenozoic Paleocyanography: Pt. 2: Biological Tracers and Biomarkers*, edited by C. Hillaire-Marcel and A. de Vernal, pp. 263–326, Elsevier, Amsterdam.
- Kaiho, K. (1994), Benthic foraminiferal dissolved-oxygen index and dissolved-oxygen levels in the modern ocean, *Geology*, 22, 719–722.

- Kaiho, K. (1999), Effect of organic carbon flux and dissolved oxygen on the benthic foraminiferal oxygen index (BFOI), *Mar. Micropaleontol.*, *37*, 67–76.
- Karstensen, J., L. Stramma, and M. Visbeck (2008), Oxygen minimum zones in the eastern tropical Atlantic and Pacific oceans, *Prog. Oceanogr.*, *77*, 331–350.
- Koho, K. A., and E. Piña-Ochoa (2012), Benthic foraminifera: Inhabitants of low-oxygen environments, in *Anoxia: Evidence for Eukaryote Survival and Paleontological Strategies: Cellular Origin, Life in Extreme Habitats, and Astrobiology 21*, edited by A. V. Altenbach, J. M. Bernhard, and J. Seckbach, pp. 251–285, Springer, Dordrecht.
- Krebs, C. J. (1999), *Ecological Methodology*, 2nd ed., Benjamin Cummings, Menlo Park, Calif.
- Levin, L. A., C. L. Huggett, and K. Wishner (1991), Control of deep-sea benthic community structure by oxygen and organic-matter gradients in the eastern Pacific Ocean, *J. Mar. Res.*, *49*, 763–800.
- Levin, L. A., J. D. Gage, C. Martin, and P. A. Lamont (2000), Macrobenthic community structure within and beneath the oxygen minimum zone, NW Arabian Sea, *Deep Sea Res., Part II*, *47*, 189–226.
- Licari, L. (2006), *Ecological Preferences of Benthic Foraminifera in the Eastern South Atlantic: Distribution Patterns, Stable Carbon Isotopic Composition, and Paleoceanographic Implications = Ökologische Ansprüche benthischer Foraminiferen im östlichen Südatlantik: Faunenverbreitung, Zusammensetzung stabiler Kohlenstoffisotope und paläozeanographische Bedeutung, Berichte zur Polar- und Meeresforschung (Reports on Polar and Marine Research)*, pp. 523, Alfred Wegener Institute for Polar and Marine Research, Bremerhaven.
- Loubere, P. (1994), Quantitative estimation of surface ocean productivity and bottom water oxygen concentration using benthic foraminifera, *Paleoceanography*, *9*, 723–737, doi:10.1029/94PA01624.
- Lynn, R. J., and J. J. Simpson (1987), The California Current System: The seasonal variability of its physical characteristics, *J. Geophys. Res.*, *92*, 12,947–12,966, doi:10.1029/JC092iC12p12947.
- Magurran, A. E. (2004), *Measuring Biological Diversity*, second ed., Blackwell Sci. Ltd, Oxford, U. K.
- Mallon, J., N. Glock, and J. Schönfeld (2012), The response of benthic foraminifera to low-oxygen conditions of the Peruvian oxygen minimum zone, in *Anoxia: Evidence for Eukaryote Survival and Paleontological Strategies: Cellular Origin, Life in Extreme Habitats, and Astrobiology 21*, edited by A. V. Altenbach, J. M. Bernhard, and J. Seckbach, pp. 305–321, Springer, Dordrecht.
- Menviel, L., A. Timmermann, A. Mouchet, O. Timm, A. Abe-Ouchi, M. O. Chikamoto, N. Harada, R. Ohgaito, and Y. Okazaki (2012), Removing the North Pacific halocline: Effects on global climate, ocean circulation and the carbon cycle, *Deep Sea Res., Part II*, *61–64*, 106–113.
- Menviel, L., M. H. England, K. J. Meissner, A. Mouchet, and J. Yu (2014), Atlantic-Pacific seesaw and its role in outgassing CO₂ during Heinrich events, *Paleoceanography*, *29*, 58–70, doi:10.1002/2013PA002542.
- Moffitt, S. E., T. M. Hill, K. Ohkushi, J. P. Kennett, and R. J. Behl (2014), Vertical oxygen minimum zone oscillations since 20 ka in Santa Barbara Basin: A benthic foraminiferal community perspective, *Paleoceanography*, *29*, 44–57, doi:10.1002/2013PA002483.
- Moffitt, S. E., R. A. Moffitt, W. Sauthoff, C. V. Davis, K. Hewett, and T. M. Hill (2015a), Paleoceanographic insights on recent oxygen minimum zone expansion: Lessons for modern oceanography, *PLoS One*, *10*, e0115246.
- Moffitt, S. E., T. M. Hill, P. D. Roopnarine, and J. P. Kennett (2015b), Response of seafloor ecosystems to abrupt global climate change, *Proc. Natl. Acad. Sci. U.S.A.*, *112*, 4684–4689.
- Morris, E. K., et al. (2014), Choosing and using diversity indices: Insights for ecological applications from the German Biodiversity exploratories, *Ecol. Evol.*, *4*, 3514–3524.
- Murdmann, I. O., G. H. Kazarina, L. Beaufort, E. V. Ivanova, E. M. Emelyanov, V. A. Kravtsov, G. N. Alekhina, and V. E. Vasileva (2010), Upper quaternary laminated sapropelic sediments from the continental slope of Baja California, *Lithol. Min. Resour.*, *45*, 154–171.
- Murray, J. W. (2006), *Ecology and Applications of Benthic Foraminifera*, Cambridge Univ. Press, Cambridge.
- Naidu, P. D., and B. A. Malmgren (1995), Do benthic foraminifer records represent a productivity index in oxygen minimum zone areas? An evaluation from the Oman Margin, Arabian Sea, *Mar. Micropaleontol.*, *26*, 49–55.
- Nameroff, T. J., L. S. Balistrieri, and J. W. Murray (2002), Suboxic trace metal geochemistry in the eastern tropical North Pacific, *Geochim. Cosmochim. Acta*, *66*, 1139–1158.
- Nederbragt, A. J., J. W. Thuroff, and P. R. Bown (2008), Paleoproductivity, ventilation, and organic carbon burial in the Santa Barbara Basin (ODP Site 893, off California) since the last glacial, *Paleoceanography*, *23*, PA1211, doi:10.1029/2007PA001501.
- Nguyen, T. M. P., M. R. Petrizzo, and R. P. Speijer (2009), Experimental dissolution of a fossil foraminiferal assemblage (Paleocene–Eocene Thermal Maximum, Dababiya, Egypt): Implications for paleoenvironmental reconstructions, *Mar. Micropaleontol.*, *73*, 241–258.
- Oberhänsli, H., P. Heinze, L. Diester-Haass, and G. Wefer (1990), Upwelling off Peru during the last 430,000 yr and its relationship to the bottom-water environment, as deduced from coarse grain-size distributions and analyses of benthic foraminifera at holes 679D, 680B, and 681B, Leg 112, in *Proceedings of the Ocean Drilling Program, Scientific Results*, vol. 112, edited by E. Suess and R. von Huene, pp. 369–390, Ocean Drilling Program, College Station, Tex.
- Ohkushi, K., J. P. Kennett, C. M. Zeleski, S. E. Moffitt, T. M. Hill, C. Robert, L. Beaufort, and R. J. Behl (2013), Quantified intermediate water oxygenation history of the northeast Pacific: A new benthic foraminiferal record from Santa Barbara Basin, *Paleoceanography*, *29*, 1–15, doi:10.1002/palo.20043.
- Ortiz, J. D., S. B. O’Connell, J. DelViscio, W. Dean, J. D. Carriquiry, T. Marchitto, Y. Zheng, and A. van Geen (2004), Enhanced marine productivity off western North America during warm climate intervals of the past 52 ky, *Geology*, *32*, 521–524.
- Ovspeyan, E. A., and E. V. Ivanova (2009), Benthic foraminiferal assemblages as indicators of the paleoceanographic conditions in the eastern equatorial Pacific, *Oceanology*, *49*, 121–129.
- Patterson, R. T., and E. Fishbein (1989), Re-examination of the statistical methods used to determine the number of point counts needed for micropaleontological quantitative research, *J. Paleontol.*, *63*, 245–248.
- Paulmier, A., and D. Ruiz-Pino (2009), Oxygen minimum zones (OMZs) in the modern ocean, *Prog. Oceanogr.*, *80*, 113–128.
- Phleger, F. L., and A. Soutar (1973), Production of benthic foraminifera in three east Pacific oxygen minima, *Micropaleontology*, *19*, 110–115.
- Praetorius, S. K., A. C. Mix, M. H. Walczak, M. D. Wilhowe, J. A. Addison, and F. G. Pahl (2015), North Pacific deglacial hypoxic events linked to abrupt ocean warming, *Nature*, *527*, 362–366.
- Rathburn, A. E., B. H. Corliss, K. D. Tappa, and K. C. Lohmann (1996), Comparisons of the ecology and stable isotopic compositions of living (stained) benthic foraminifera from the Sulu and South China Seas, *Deep Sea Res., Part I*, *43*, 1617–1646.
- Rodriguez-Sanz, L., P. G. Mortyn, J. C. Herguera, and R. Zahn (2013), Hydrographic changes in the tropical and extratropical Pacific during the last deglaciation, *Paleoceanography*, *28*, 529–538, doi:10.1002/palo.20049.
- Schlitzer, R. (2017), Ocean data view. [Available at www.odv.awi.de]
- Schmiedl, G., A. Mackensen, and P. J. Müller (1997), Recent benthic foraminifera from the eastern South Atlantic Ocean: Dependence on food supply and water masses, *Mar. Micropaleontol.*, *32*, 249–287.

- Schmittner, A., E. D. Galbraith, S. W. Hostetler, T. F. Pederson, and R. Zhang (2007), Large fluctuations of dissolved oxygen in the Indian and Pacific Oceans during Dansgaard-Oeschger oscillations caused by variations of North Atlantic Deep Water subduction, *Paleoceanography*, *22*, PA3207, doi:10.1029/2006PA001384.
- Scholz, F., J. McManus, A. C. Mix, C. Hensen, and R. R. Schneider (2014), The impact of ocean deoxygenation on iron release from continental margin sediments, *Nat. Geosci.*, *7*, 433–437.
- Schumacher, S., F. J. Jorissen, D. Dissard, K. E. Larkin, and A. J. Gooday (2007), Live (Rose Bengal stained) and dead benthic Foraminifera from the oxygen minimum zone of the Pakistan continental margin (Arabian Sea), *Mar. Micropaleontol.*, *62*, 45–73.
- Sen Gupta, B. K., and M. L. Machain-Castillo (1993), Benthic Foraminifera in oxygen-poor habitats, *Mar. Micropaleontol.*, *20*, 183–201.
- Sigman, D. M., A. M. De Boer, and G. H. Haug (2007), Antarctic stratification, atmospheric water vapor, and Heinrich events: A hypothesis for late Pleistocene deglaciations, in *Ocean Circulation: Mechanisms and Impacts*, AGU Geophys. Monogr., vol. 173, edited by A. Schmittner, J. C. H. Chiang, and S. R. Hemming, pp. 335–349, AGU, Washington, D. C.
- Stewart, R. E., and K. C. Stewart (1930), Post-Miocene foraminifera from the Ventura Quadrangle, Ventura County, California: Twelve new species of varieties from the Pliocene, *J. Paleontol.*, *4*, 60–72.
- Stramma, L., G. C. Johnson, J. Sprintall, and V. Mohrholz (2008), Expanding oxygen-minimum zones in the tropical oceans, *Science*, *320*, 655–658.
- Timmermann, A., U. Krebs, F. Justino, H. Goosse, and T. Ivanochko (2005), Mechanisms for millennial-scale global synchronization during the last glacial period, *Paleoceanography*, *20*, PA4008, doi:10.1029/2004PA001090.
- Tribouillard, N., T. J. Algeo, T. Lyons, and A. Riboulleau (2006), Trace metals as paleoredox and paleoproductivity proxies: An update, *Chem. Geol.*, *232*, 12–32.
- Van der Weijden, C., G. Reichert, and B. Vanos (2006), Sedimentary trace element records over the last 200 kyr from within and below the northern Arabian Sea oxygen minimum zone, *Mar. Geol.*, *231*, 68–88.
- Van der Zwaan, G. J., I. A. P. Duijnste, M. den Dulk, S. R. Ernst, N. T. Jannink, T. J. Kouwenhoven (1999), Benthic foraminifers: proxies or problems? A review of paleocological concepts, *Earth-Sci. Rev.*, *46*, 213–236.
- van Geen, A., A. Horneman, W. M. Smethie Jr., and H. Lee (2006), Sensitivity of the North Pacific oxygen minimum zone to changes in ocean circulation: A simple model calibrated by chlorofluorocarbons, *J. Geophys. Res.*, *111*, C10004, doi:10.1029/2005JC003192.
- Wyrski, K. (1962), The oxygen minima in relation to ocean circulation, *Deep Sea Res. Oceanic Abstr.*, *9*, 11–23.
- Zheng, Y., A. van Geen, R. F. Anderson, J. V. Gardner, and W. E. Dean (2000), Intensification of the northeast Pacific oxygen minimum zone during the Bolling–Allerod warm period, *Paleoceanography*, *15*, 528–536, doi:10.1029/1999PA000473.